Nitrile butadiene rubber composites reinforced with reduced graphene oxide and carbon nanotubes show superior mechanical, electrical and icephobic properties

L. Valentini [a], [*], S. Bittolo Bon [a], M. Hernández [b], M.A. Lopez-Manchado [b], [**], N.M. Pugno [c], [d], [e]

[a] Civil and Environmental Engineering Department, University of Perugia, UdR INSTM, Strada di Pentima 4, 05100 Terni, Italy
[b] Instituto de Ciencia y Tecnología de Polímeros, ICTP-CSIC, Juan de la Cierva, 3, 28006 Madrid, Spain
[c] Laboratory of Bio-Inspired and Graphene Nanomechanics, Department of Civil, Environmental and Mechanical Engineering, University of Trento, Trento, Italy
[d] School of Engineering and Materials Science, Queen Mary University of London, Mile End Road, London, United Kingdom
[e] Ket Lab, Edoardo Amaldi Foundation, Italian Space Agency, via del Politecnico snc, I-00133 Roma, Italy

ARTICLE INFO

ABSTRACT

In this article, we examine the effects of two different nanostructured carbons when they are incorporated in a rubber matrix in terms of mechanical and electrical properties as well as the icephobic behaviour of the nanocomposites when swollen. Nitrile butadiene rubber composites reinforced with thermally reduced graphene oxide or multiwalled carbon nanotubes or both of them were prepared and characterized. At a particular hybrid filler loading, tensile and electrical tests showed a significant improvement of the composite. From the swelling studies, after the immersion, the nanocomposites experienced a reduction of the cross-link density that promotes weakening of ice adhesion, being this effect more evident for those samples prepared with hybrid fillers. In view of the composite formulations, that utilize commercially available elastomers and fillers, these findings would be applicable to the automotive and aviation sectors, where the demand for multifunctional rubbers is increasing.

© 2018 Elsevier Ltd. All rights reserved.

1. Introduction

Nanocarbons such as carbon nanotubes (CNTs) and graphene nanoplatelets exhibit superior mechanical and electrical properties compared to other nanofillers, making them ideal candidates as fillers for polymer nanocomposites used in advanced applications [1–5]. Thus, an important use of such nanomaterials is in reinforcing polymer matrices taking advantage of the ultra-high stiffness and electrical conductivity exhibited by them. The nanotube dispersion and deformation mechanisms in polymer composites were addressed by Qian et al. [6] who studied a model composite system in which carbon nanotubes were dispersed in a polystyrene matrix. Xie et al. [7] predicted theoretically that graphene is more

effective for electrical conductivity than CNTs because of its large specific surface area even if, in this regard, there are contradictory studies stating that graphene is less effective than CNTs in forming conductive percolated networks [8].

Some of the recent researches have combined CNTs with other fillers. Prasad et al. [9] reported the synergy effect in the mechanical properties of polymer matrix composites when reinforced with two different nanocarbons. It was also found that graphene and CNTs enhanced the mechanical properties of silicone rubber [10]; Bokobza et al. [11] reported the stress-strain improvement in styrene–butadiene rubber when a blend of carbon black and CNTs were used, while Valentini et al. [12] reported the synergistic effect of graphene nanoplatelets and carbon black in EPDM nanocomposites. Other findings showed how hybrid carbon nanofillers had synergistic effects in electrical conductivity, thermal conductivity and mechanical properties [13–15].

These graphitic compounds (CNTs, graphene), compared to other conventional types of fillers, exhibit a significant ability to enhance mechanical and other functional properties of a rubber-

like matrix, especially in the case of fine dispersion in the host medium, which acts in favour of the enhanced interfacial interaction [16–18]. Nitrile butadiene rubber (NBR) is commonly considered the workhorse of the industrial and automotive rubber products because of its good mechanical properties, its resistance to lubricants and greases and its relatively low cost [19,20]. Efforts also have to be done to find more suitable filler for NBR in order to achieve high performance products with higher tensile strength and electrical conductivity, being the mechanisms behind the synergetic effects of hybrid fillers in this matrix not completely understood [21–23]. There is a need to develop high performance elastomeric materials in extreme environments; for example, there is now, and will continue to be, a need to develop high performance elastomeric sealing materials for oil and gas applications for primary use in the exploration and operational drilling applications, in ever unexplored locations of the northern hemisphere; this makes the icing issue challenging. In such extreme conditions, icing problems will become more hazardous, limiting activities at oil and gas extraction unless reliable solutions are found [24].

In the frame of the presented work, NBR composites were prepared using thermally reduced graphene oxide (TRGO) or CNTs or both of them (hybrid, i.e. TRGO + CNTs) as fillers. We were also interested in investigating the physical properties and swelling of neat NBR and respective TRGO/CNT composites and in understanding their surface adhesion properties with specific attention to ice.

2. Experimental details

NBR under the trade name Krynac 2850 F (acrylonitrile content: 27.5 wt%, Mooney viscosity M_L (1 + 4) 100 °C 48 and a density of 0.97 g/cm^3) was used as rubber matrix. TRGO was synthetized in our laboratories following the procedures described elsewhere [25]. CNTs were kindly supplied by Nanocyl S.A. under the trade name Nanocyl NC7000.

Rubber compounds were prepared in an open two-roll mill at room temperature. The rotors operated at a speed ratio of 1:1.4. The vulcanization ingredients were sequentially added to the rubber before to the incorporation of the filler and sulphur. The recipes of the compounds are described in Table 1. Vulcanizing conditions (temperature and time) were previously determined by a Monsanto Moving Die Rheometer MDR 2000E. Rubber compounds were then vulcanized at 160 °C in a thermofluid heated press. The vulcanization time of the samples corresponds to the optimum cure time t$_{90}$ derived from the curing curves of the MDR 2000E.

The filler volume fraction was calculated from the well-known relationship:

$$f = (W_f/\rho_f)/(W_f/\rho_f + W_m/\rho_m) \tag{1}$$

where W_f is the weight fraction of the filler and W_m is the weight fraction of the matrix, while ρ_f and ρ_m are the densities of the filler (i.e. 1.75 g/cm^3 for CNTs [26,27] and 2.2 g/cm^3 for TRGO [28]) and of the matrix, respectively. For the case of the hybrid filler, the equation was trivially extended in order to take into account the presence of both fillers in the matrix volume.

Tensile stress-strain properties were measured according to ISO 37-1977 specifications, on an Instron dynamometer (Model 4301), at 25 °C at a crosshead speed of 500 mm min^{-1}. At least five specimens of each sample type were tested. The samples were then cut into strips of ~100 mm × 20 mm × 0.13 mm, the electrical resistance was measured using a computer controlled Keithley 4200 source. The electrical resistance measurements were performed by biasing the sample between two strips of silver paint located at a distance of 25 mm.

Trans-1,2-dichloroethylene was used as fluid for immersion. The specimens have been immersed in the fluid for 70 h at the temperatures of 25 °C. Test procedure was in accordance with ASTM D 471; at the end of the required immersion period, the specimens were cooled down to room temperature for 30–60 min, then dipped quickly in acetone at room temperature, and blot lightly with filter paper. The swelling studies were performed on a known volume and weight of vulcanized rubber in the form of a rectangular sample that was taken for swelling measurements in immersion liquids. After attaining equilibrium swelling (70 h), its weight was recorded and the volume variation was estimated according to ASTM D 471. The "ice adhesion strength" was measured using a custom setup, where a force transducer was fixed to a slipping table, as the maximal shear force needed to delaminate the ice agglomerate divided by its contact area with the NBR (thus it is just an indication of the mean value of the ultimate shear stress under the testing conditions, Table 2). Prisms with the dimension of 10 mm × 10 mm × 6 mm were positioned on the sample surface and then filled with water. They were then frozen 12 h at −20 °C. The shear force was applied at a distance of 1 mm about the prism-elastomer interface. Testing was done at −10 °C.

3. Results and discussion

The mechanical properties of the samples filled with CNTs, TRGO and hybrid fillers were evaluated by tensile testing (Fig. 1a−b) and the results are summarized in Tables 2 and 3. The addition of the TRGO and CNTs as a sole reinforcement as well as the addition of both of them causes a sensible increase of the stress at several elongations, tensile strength and fracture strength of the NBR composites. The reinforcing effect of both nanoparticles is more marked as the elongation is increased, reaching improvements of the tensile strength of 150 and 315% for nanocomposites containing 5 phr of TRGO or CNTs, respectively. In addition, this

Table 1
Recipes of the rubber compounds (indicated in phr: parts per hundred of rubber).

Sample (TRGO/CNTs)	NBR	ZnO	Stearic acid	MBT	S	TRGO	CNT
0/0	100	5	1.5	1.5	1.5	0.0	0.0
1/0	100	5	1.5	1.5	1.5	1.0	0.0
3/0	100	5	1.5	1.5	1.5	3.0	0.0
5/0	100	5	1.5	1.5	1.5	5.0	0.0
0/1	100	5	1.5	1.5	1.5	0.0	1.0
0/3	100	5	1.5	1.5	1.5	0.0	3.0
0/5	100	5	1.5	1.5	1.5	0.0	5.0
0.5/0.5	100	5	1.5	1.5	1.5	0.5	0.5
1.5/1.5	100	5	1.5	1.5	1.5	1.5	1.5
2.5/2.5	100	5	1.5	1.5	1.5	2.5	2.5
1/5	100	5	1.5	1.5	1.5	1.0	5.0
5/1	100	5	1.5	1.5	1.5	5.0	1.0

Table 2
Filler volume fraction (*f*) and filler equivalent strengths of the prepared composites.

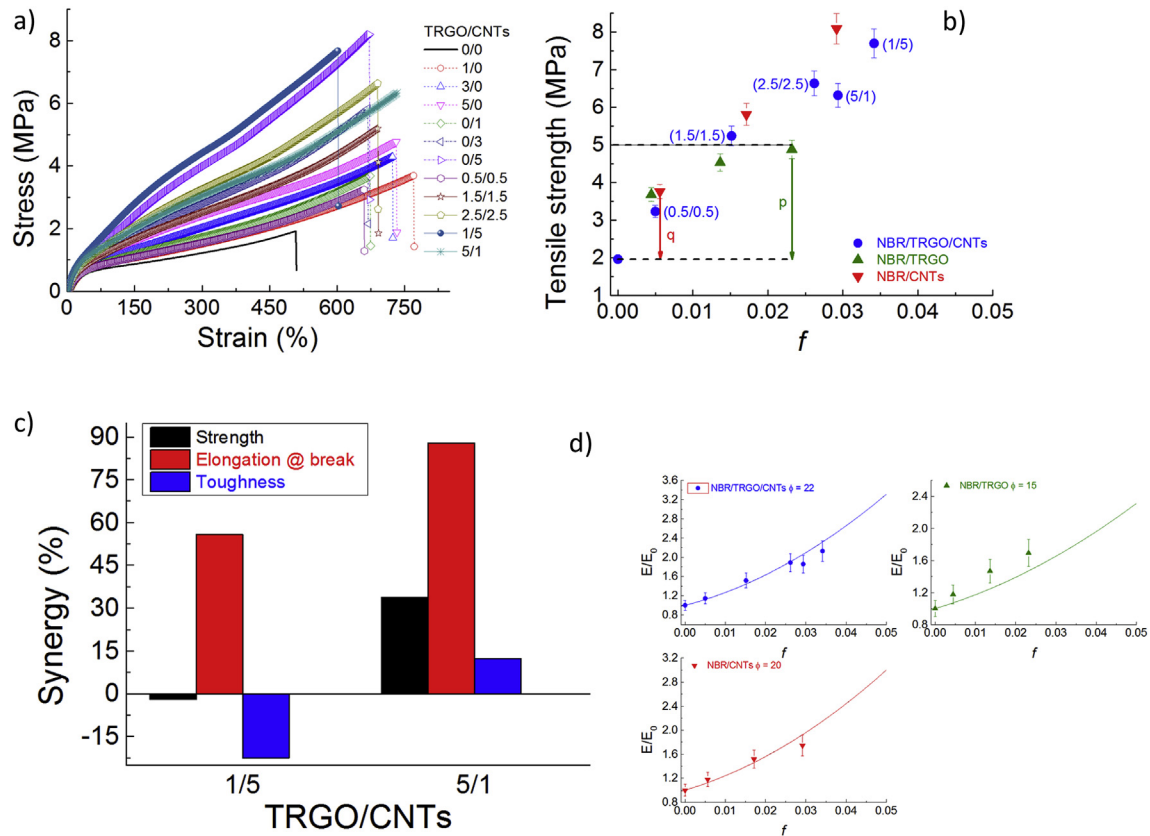| Sample (TRGO/CNTs)	*f*	Filler equivalent strength (MPa)
0/0	0	—
1/0	0.0044	388.48
3/0	0.014	190.38
5/0	0.023	127.77
0/1	0.0056	323.39
0/3	0.017	226.58
0/5	0.029	212.11
0.5/0.5	0.005	255.96
1.5/1.5	0.015	218.32
2.5/2.5	0.026	180.65
1/5	0.034	169.94
5/1	0.029	150.51

Fig. 1. (a) Stress-strain curves and (b) tensile strength of the NBR composites filled with different types of nanostructured carbon fillers. The hybrid filler composition (TRGO/CNTs) in phr (parts per hundred rubber) is also indicated. (c) Percentage synergy in strength, elongation at break and toughness for two different binary composites. (d) Plot of reduced elastic modulus of the NBR composites filled with different types of carbon nanomaterials measured at low strain (i. e. 50%). The solid lines are the fitted curves evaluated according to eq. (3).

Table 3
Mechanical properties of NBR compounds.

Sample (TRGO/CNTs)	Stress 50% elongation (MPa)	Stress 100% elongation (MPa)	Stress 300% elongation (MPa)	Stress 500% elongation (MPa)	Max Strength (MPa)	Elongation at break (%)	Toughness (MPa)
0/0	0.62 ± 0.02	0.78 ± 0.02	1.23 ± 0.03	1.89 ± 0.04	1.96 ± 0.11	508 ± 43	4.97 ± 0.10
1/0	0.73 ± 0.01	0.93 ± 0.01	1.51 ± 0.01	2.26 ± 0.02	3.68 ± 0.39	756 ± 66	13.91 ± 0.13
3/0	0.91 ± 0.02	1.16 ± 0.03	2.08 ± 0.05	3.03 ± 0.07	4.53 ± 0.42	739 ± 43	16.73 ± 0.10
5/0	1.05 ± 0.02	1.35 ± 0.03	2.44 ± 0.07	3.36 ± 0.11	4.88 ± 0.57	735 ± 61	17.93 ± 0.14
0/1	0.73 ± 0.01	0.99 ± 0.01	1.75 ± 0.02	2.63 ± 0.04	3.76 ± 0.26	671 ± 38	12.61 ± 0.09
0/3	0.94 ± 0.02	1.41 ± 0.05	2.90 ± 0.10	4.30 ± 0.21	5.81 ± 0.32	647 ± 39	18.79 ± 0.08
0/5	1.08 ± 0.01	1.69 ± 0.01	3.89 ± 0.02	5.93 ± 0.04	8.09 ± 0.26	670 ± 41	26.37 ± 0.07
0.5/0.5	0.71 ± 0.03	0.93 ± 0.06	1.54 ± 0.11	2.30 ± 0.16	3.23 ± 0.47	652 ± 29	10.82 ± 0.15
1.5/1.5	0.94 ± 0.02	1.33 ± 0.04	2.50 ± 0.07	3.63 ± 0.10	5.24 ± 0.63	693 ± 22	18.15 ± 0.12
2.5/2.5	1.17 ± 0.04	1.76 ± 0.09	3.26 ± 0.10	5.06 ± 0.22	6.64 ± 0.33	672 ± 33	22.31 ± 0.07
1/5	1.32 ± 0.06	2.10 ± 0.12	4.43 ± 0.16	6.53 ± 0.18	7.70 ± 0.18	611 ± 24	23.52 ± 0.05
5/1	1.15 ± 0.02	1.59 ± 0.03	3.05 ± 0.05	4.24 ± 0.07	6.32 ± 0.60	733 ± 61	23.16 ± 0.13

improvement does not imply a deterioration of the elastic properties of the material: all nanocomposites exhibit a higher elongation at break in relation to pristine rubber. It was found that the two fillers usually do not act in synergy here with respect to strength, see Table 2, where the equivalent strength of the filler is estimated from a classical direct rule of mixture.

Note that the addition of 5 phr TRGO alone to NBR leads to an enhancement in tensile strength of NBR by p as shown in Fig. 1b. Likewise, q represents the enhancement in tensile strength of NBR due to the addition of 1 phr CNTs alone in Fig. 1b. The synergistic effect or percent synergy attained by adding both 5 phr TRGO and 1 phr CNTs to NBR can also be computed as suggested by Prasad et al.

[9] by the following relation:

$$[M_h-(p + q)]*100/(p + q) \qquad (2)$$

where M_h is the measured value for the related composite, Fig. 1c, for strength, elongation at break and toughness. The positive value of the synergy also for the strength for the hybrid 5/1 is due to the different definition with respect to the previous approach based on the filler equivalent strength, as reported in Table 2.

The most direct evaluation of the influence of filler particles on the mechanical response of elastomers is to consider the small strain modulus versus volume fraction fillers, as shown in Fig. 1 (d).

The solid lines are the curves fitted to the Guth-Gold-Smallwood model [29], that for filled elastomeric system predicts the enhancement of the initial modulus according to the following equation:

$$E/E_0 = 1 + 0.67f\phi + 1.62f^2\phi^2 \qquad (3)$$

where, E and E_0 are the moduli of filled and unfilled elastomers, respectively, f is the filler volume fraction and ϕ is the shape effect factor. The quadratic term takes into account the particle aggregation (clustering) and also allows the application of the equation to non-spherical fillers, particularly when the fillers are either platelet like structure or rod like structure like in our case. The ϕ value (i.e. 22) for the hybrid composites was found higher than those observed for the single phase composites (i.e. 15 for both TRGO and 20 for CNTs) indicating a higher contribution to the modulus due to the better dispersion of either CNTs by disentanglement of the bundle or delamination of the TRGO. This simple analysis is interesting for the processing point of view; CNTs are, for most polymers, more reinforcing than graphene, leading to better mechanical properties and higher electrical conductivity values [30,31]. On the other hand, the advantage of graphene relies on the fact that it does not increase much the polymer viscosity; so, having the proof of the concept that with the hybrid formulation we get a better dispersion, it could be easier to process the polymers allowing the incorporation of higher volume fractions.

The ratio of the volume fraction of the swollen rubber (V_0) and swollen filled rubber (V_f), respectively, has a direct relationship with the crosslink of the filler with the rubber matrix and thus estimates the interaction of the filler and matrix. Fig. 2 shows the plot of V_0/V_f against $f/(1-f)$ according to Kraus equation [32]:

$$V_0/V_f = 1 - m\,f/(1-f) \qquad (4)$$

where f is the volume fraction of the filler in the vulcanized rubber, m represents the polymer-filler interaction parameter, obtained from the opposite (in sign) of the slope of the plot of (V_0/V_f-1) against $f/(1-f)$: the higher the m value, the better the polymer−filler interaction [33]. This can also be seen in Fig. 2, where the Kraus plot of single phase and hybrid composites are reported. According to these results, the hybrid fillers have the slope similar to that of single phase composites, indicating a similar rubber−filler interaction, even if the (5/1) solution appears as the best.

Fig. 3 shows the electrical conductivity dependence on filler loading for the prepared nanocomposites. With a graphene loading
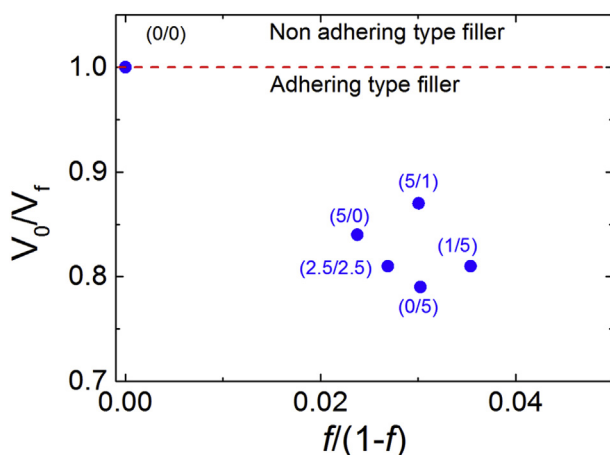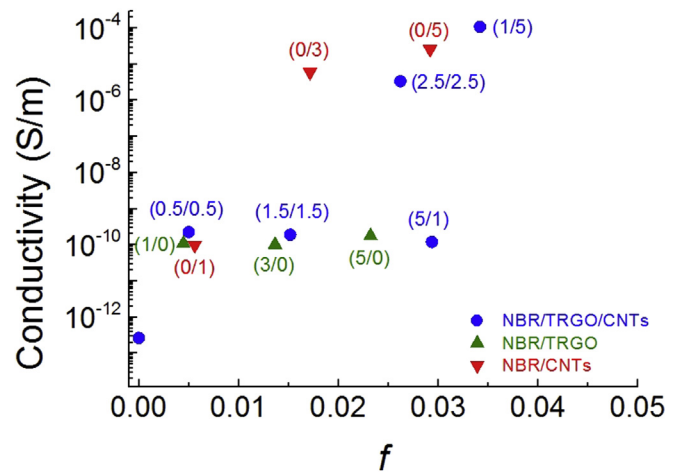

Fig. 3. Electrical conductivity of the nanocomposites as a function of filler volume fraction.

of $f = 0.02$, the electrical conductivity was about 4.3×10^{-10} S/m. At the CNT volume fraction of 0.017, the conductivity was 6×10^{-6} S/m, which already exceeds the common value for surpassing the antistatic criterion, namely 10^{-6} S/m. Interestingly, for the hybrid composites we observed a rise of the conductivity to 1×10^{-4} S/m with a filler content of $f = 0.034$, which corresponds to the hybrid formulation 1/5. The aspect ratio of the fillers is the most important factor affecting the percolation threshold, that would decrease with increasing aspect ratio. The effect of aspect ratio can be explained by the excluded volume theory. The excluded volume is defined as the volume around an object into which the center of another similar object is not allowed to enter if interpenetration of the two objects has to be avoided. Thus, a higher aspect ratio induces a larger excluded volume, and thus lowers the percolation threshold. The conductive percolation threshold (ϕ_p) can be related to the aspect ratio (A_f) by the following equation [34−37]:

$$A_f = 3\phi_{sphere}/(2\phi_p) \qquad (5)$$

where $\phi_{sphere} = 0.30$ is a factor assuming the interaction of layered structures with an excluded volume assimilated to 3D percolating spheres [38]. Substituting in Eq. (5) the percolation volume fraction reported in Fig. 3 we estimated an increase of the aspect ratio from 26 to 102 passing from the NBR/CNTs to NBR/TRGO composite, respectively. This means that the excluded volume of a network of TRGO is higher than that of a network of CNTs, suggesting a more densely packed network for CNTs in the hybrid composition.

In the case of vulcanized rubbers, the polymer consists of a network structure of cross-linked chains that limit the amount of liquid that can be absorbed. Thus the greater the number of cross

Fig. 2. Kraus' plot for composites with various fillers.

Table 4

Nanocomposites reported in Table 1 and resulting swelling ratios, liquid volume fraction (Φ_{LIQUID}) before and after liquid immersion and molecular weight M_c between cross-links. The properties are after the immersion in *trans*-1,2-dichloroethylene.

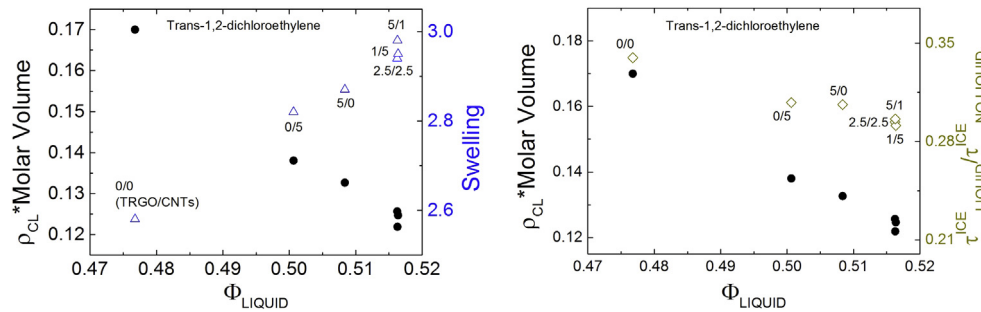| TRGO/CNTs	Swelling	Φ_{LIQUID}	M_c (g/mol)
0/0	2.58	0.477	781
5/0	2.82	0.500	889
0/5	2.87	0.508	924
2.5/2.5	2.94	0.516	953
1/5	2.95	0.516	967
5/1	2.98	0.516	983

Fig. 4. (a) Swell ratio (triangles) and cross-link density reduction (circles) of liquid-filled TRGO/CNTs nanocomposites as a function of the liquid volume fraction. (b) Comparison with measured ice adhesion strength ratio (rhombs) for NBR nanocomposites obtained with different TRGO/CNTs combinations as a function of the liquid volume fraction.

bonds in the elastomer the less it will swell. The swelling is thus an equilibrium state obtained when the dimensions of the elastomer increase until the concentration of the liquid is uniform throughout the component [39]. This relationship is quantitatively expressed by the Flory-Rehner equation [40,41]:

$$\rho_{CL} = [\ln(1-V_r)+V_r+\chi V_r^2]/[V(V_r^{1/3}-0.5V_r)] \tag{6}$$

where the ρ_{CL} is the cross-linking density, V_r is the volume fraction of polymer in a swollen state, χ is the Flory-Huggins interaction parameter between the polymer and the solvent and V is the molar volume of the solvent.

According to the Flory and Rehner theory [42], originally derived for natural rubber vulcanized with carbon black assuming that rigid fillers within the elastic network would not swell in the presence of a solvent, we calculate the volume fraction of the liquid within the swollen elastomers from the well-known relationship:

$$\Phi_{LIQUID}=(W_{LIQUID}/\rho_{LIQUID})/(W_{LIQUID}/\rho_{LIQUID} + f + W_m/\rho_m) \tag{7}$$

where W_{LIQUID} is the weight fraction of the liquid calculated from the relative difference of the weights of the sample in its dry and swollen state, f is the volume fraction of the filler and W_m is the weight fraction of the matrix, while ρ_{LIQUID} and ρ_m are the densities of the liquid and polymer matrix respectively. For large values of swelling, S, (i.e. small values of $\nu = 1/S$), the molecular weight per chain (M_c) can be expressed as [41]:

$$M_c \sim 2\rho V/(\nu)^{5/3} \tag{8}$$

where ρ is the polymer density. Eq. (8) states that the molecular weight between cross-links will increase with increasing the swelling; applying this equation to the high swollen state of TRGO/CNT composites in *trans*-1,2-dichloroethylene, the values of M_c were calculated and reported in Table 4. In Fig. 4a, we show the relationship between the swelling and the cross-link density; the data indicate how a certain amount of liquid reduces the cross-link density of the prepared composites.

Ice adhesion mechanisms at polymer interface can be at least roughly understood if we idealize the elastomer as a 'connector molecules' [42], that is, polymer chains are bound to the interface by physisorbtion, and interact with the bulk polymer so that they act to transmit stress across the interface. Assuming that during the ice detachment a chain with n monomers of size a is partially extracted, we could associate this with the pull-out energy proposed by de Gennes et al. [43], where the free energy is a combination of the surface energy required to extract the chain and the elastic energy associated with the stretching of the extracted portion of the chain. Assuming the adhesion strength proportional

to the surface tension that rescales with the inverse of the n^*a (i. e. M_c) [31], we find a good matching between the cross-link density and the results reported in Fig. 4b where we present the ice adhesion data for the prepared nanocomposites after liquid immersion, where τ^{ice}_{liquid} is the adhesion strength of liquid filled sample while $\tau^{ice}_{no\ liquid}$ is the adhesion strength of the unfilled sample. In particular, we observed the reduction of the ice adhesion strength ratio between the swollen and unswollen TRGO/CNTs/NBR nanocomposite with the decrease (increase) of the cross-link density (molecular weight per chain).

4. Conclusions

The mechanical strength and electrical conductivity of NBR composites containing independent or hybrid fillers of TRGO and CNTs were investigated. The results suggested that there are optimal concentrations of nanofillers for achieving the maximum strength and electrical conductivity of the composites. Materials with the highest reduction of the cross-link density show a lowest interfacial interaction. A hybrid TRGO/CNTs system decreases the ice adhesion strength of the rubber material. We rationalized such results calculating the molecular weight between cross-links, and the adhesion strength according to the adhesion mechanisms at soft polymer interfaces, that can be modelled in terms of relays of dissipation mechanisms acting at different length scales, from molecular to macroscopic. We foresee such rubber nanocomposites having applications in several industrial areas where rubber based components need to operate in extreme environments.

References

[1] V. Kostopoulos, A. Vavouliotis, P. Karapappas, P. Tsotra, A. Paipetis, Damage monitoring of carbon fiber reinforced laminates using resistance measurements. Improving sensitivity using carbon nanotube doped epoxy matrix system, J. Intell. Mater. Syst. Struct. 20 (2009) 1025–1034.
[2] E. Badamshina, Y. Estrin, M. Gafurova, Nanocomposites based on polyurethanes and carbon nanoparticles: preparation, properties and application, J. Mater. Chem. 1 (2013) 6509–6529.
[3] J.R. Potts, D.R. Dreyer, C.W. Bielawski, R.S. Ruoff, Graphene-based Polymer Nanocomposites Polymer, vol 52, 2011, pp. 5–25.
[4] D. Cai, M. Song, Recent advance in functionalized graphene/polymer nanocomposites, J. Mater. Chem. 20 (2010) 7906–7915.
[5] R. Verdejo, M.M. Bernal, J. Laura, L.J. Romasanta, M.A. Lopez-Manchado,

Graphene filled polymer nanocomposites, J. Mater. Chem. 21 (2011) 3301–3310.

[6] D. Qian, E.C. Dickey, R. Andrews, T. Rantell, Load transfer and deformation mechanisms in carbon nanotube-polystyrene composites, Appl. Phys. Lett. 76 (2000) 2868–2870.

[7] S. Xie, Y. Liu, J.Y. Li, Comparison of the effective conductivity between composites reinforced by graphene nanosheets and carbon nanotubes, Appl. Phys. Lett. 92 (2008) 243121–243123.

[8] J.H. Du, L. Zhao, Y. Zeng, L.L. Zhang, F. Li, P.F. Liu, Comparison of electrical properties between multi-walled carbon nanotube and graphene nanosheet/high density polyethylene composites with a segregated network structure, Carbon 49 (2011) 1094–1100.

[9] K.E. Prasad, B. Das, U. Maitra, U. Ramamurty, C.N.R. Rao, Extraordinary synergy in the mechanical properties of polymer matrix composites reinforced with 2 nanocarbons, Proc. Natl. Acad. Sci. U.S.A. 1060 (2009) 13186–13189.

[10] H. Hu, L. Zhao, J. Liu, Y. Liu, J. Cheng, J. Luo, et al., Enhanced dispersion of carbon nanotube in silicone rubber assisted by graphene, Polymer 53 (2012) 3378–3385.

[11] L. Bokobza, M. Rahmani, C. Belin, J.L. Bruneel, N.E. El Bounia, Blends of carbon blacks and multiwall carbon nanotubes as reinforcing fillers for hydrocarbon rubbers, J. Polym. Sci. 46 (2008) 1939–1951.

[12] L. Valentini, S. Bittolo Bon, M.A. Lopez-Manchado, R. Verdejo, L. Pappalardo, A. Bolognini, et al., Synergistic effect of graphene nanoplatelets and carbon black in multifunctional EPDM nanocomposites, Compos. Sci. Technol. 128 (2016) 123–130.

[13] S. Chatterjee, F. Nafezarefi, N.H. Tai, L. Schlagenhauf, F.A. Nüesch, B.T.T. Chu, Size and synergy effects of nanofiller hybrids including graphene nanoplatelets and carbon nanotubes in mechanical properties of epoxy composites, Carbon 50 (2012) 5380–5386.

[14] S. Maiti, N.K. Shrivastava, S. Suin, B.B. Khatua, Polystyrene/MWCNT/graphite nanoplatelet nanocomposites: efficient electromagnetic interference shielding material through graphite nanoplate-MWCNT-graphite nanoplate networking, ACS Appl. Mater. Interfaces 5 (2013) 4712–4724.

[15] S.Y. Yang, W.N. Lin, Y.L. Huang, H.W. Tien, J.Y. Wang, C.C.M. Ma, et al., Synergetic effects of graphene platelets and carbon nanotubes on the mechanical and thermal properties of epoxy composites, Carbon 49 (2011) 793–803.

[16] M.D. Frogley, D. Ravich, H.D. Wagner, Mechanical properties of carbon nanoparticle-reinforced elastomers, Compos. Sci. Technol. 63 (2003) 1647–1654.

[17] H. Koerner, G. Price, N. Pearce, M. Alexander, R.A. Vaia, Remotely actuated polymer nanocomposites–stress-recovery of carbon-nanotube-filled thermoplastic elastomers, Nat. Mater. 3 (2004) 115–120.

[18] A.M. Shanmugharaj, J.H. Bae, K.Y. Lee, W.H. Noh, S.H. Lee, S.H. Ryu, Physical and chemical characteristics of multiwalled carbon nanotubes functionalized with aminosilane and its influence on the properties of natural rubber composites, Compos. Sci. Technol. 67 (2007) 1813–1822.

[19] B. Alcock, J.K. Jørgensen, The mechanical properties of a model hydrogenated nitrile butadiene rubber (HNBR) following simulated sweet oil exposure at elevated temperature and pressure, Polym. Test. 46 (2015) 50–58.

[20] C. Wrana, K. Reinartz, H.R. Winkelbach, Therban® the high performance elastomer for the new millennium, Macromol. Mater. Eng. 286 (2001) 657–662.

[21] H. Aguilar-Boladosa, M. Yazdani-Pedrama, A. Contreras-Cida, M.A. López-Manchado, A. May-Pat, F. Avilés, Influence of the morphology of carbon nanostructures on the piezoresistivity of hybrid natural rubber nanocomposites, Compos. B Eng. 109 (2017) 147–154.

[22] D. Ponnamma, K.K. Sadasivuni, M. Strankowskic, Q. Guo, S. Thomas,

Synergistic effect of multi walled carbon nanotubes and reduced graphene oxides in natural rubber for sensing application, Soft Matter 9 (2013) 10343–10353.

[23] B. Pradhan, S.K. Srivastava, Synergistic effect of three-dimensional multi-walled carbon nanotube–graphene nanofiller in enhancing the mechanical and thermal properties of high-performance silicone rubber, Polym. Int. 63 (2014) 1219–1228.

[24] A. Belani, S. Orr, A systematic approach to hostile environments, J. Petrol. Technol. 60 (2008) 34–39.

[25] H. Aguilar-Bolados, M.A. Lopez-Manchado, J. Brasero, F. Aviles, M. Yazdani-Pedram, Effect of the morphology of thermally reduced graphite oxide on the mechanical and electrical properties of natural rubber nanocomposites, Composites Part B 87 (2016) 350–356.

[26] B. Krause, M. Mende, P. Pötschke, G. Petzold, Dispersability and particle size distribution of CNTs in an aqueous surfactant dispersion as a function of ultrasonic treatment time, Carbon 48 (2010) 2746–2754.

[27] Ch Laurent, E. Flahaut, A. Peigney, The weight and density of carbon nanotubes versus the number of walls and diameter, Carbon 48 (2010) 2994–2996.

[28] C. Gao, S. Zhang, F. Wang, B. Wen, C. Han, Y. Ding, et al., Graphene networks with low percolation threshold in abs nanocomposites: selective localization and electrical and rheological properties, ACS Appl. Mater. Interfaces 6 (2014) 12252–12260.

[29] E. Guth, Theory of filler reinforcement, J. Appl. Phys. 16 (1945) 20–25.

[30] A. Das, G.R. Kasaliwal, R. Jurk, R. Boldt, D. Fischer, K.W. Stöckelhuber, G. Heinrich, Rubber composites based on graphene nanoplatelets, expanded graphite, carbon nanotubes and their combination: a comparative study, Compos. Sci. Technol. 72 (2012) 1961–1967.

[31] S. Mondal, Elastomer reinforcement by graphene nanoplatelets and synergistic improvements of electrical and mechanical properties of composites by hybrid nano fillers of graphene-carbon black & graphene-MWCNT, Composites Part A 102 (2017) 154–165.

[32] G. Kraus, Swelling of filler-reinforced vulcanizates, J. Appl. Polym. Sci. 7 (1963) 861–871.

[33] K.T. Paul, S.K. Pabi, K.K. Chakraborty, G.B. Nanodi, Nanostructured fly ash–styrene butadiene rubber hybrid nanocomposites, Polym Comp 30 (2009) 1647–1656.

[34] S.I. White, R.M. Mutiso, P.M. Vora, D. Jahnke, S. Hsu, J.M. Kikkawa, et al., Electrical percolation behavior in silver nanowire–polystyrene composites: simulation and experiment, Adv. Funct. Mater. 20 (2010) 2709–2716.

[35] H. Kim, C.W. Macosko, Processing-property relationships of polycarbonate/graphene composites, Polymer 50 (2009) 3797–3809.

[36] A.P. Philipse, The random contact equation and its implications for (Colloidal) rods in packings, suspensions, and anisotropic powders, Langmuir 12 (1996), 1127e33.

[37] V.K.S. Shante, S. Kirkpatrick, An introduction to percolation theory, Adv. Phys. 20 (1971) 325–357.

[38] M.B. Isichenko, Rev. Mod. Phys. 64 (1992) 961.

[39] B.B. Boonstra, in: C.M. Blow, C. Hepburn (Eds.), Rubber Technology and Manufacture, Newnes-Butterworths, London (, 1975.

[40] P.J. Flory, J. Rehner Jr., Statistical mechanics of cross-linked polymer networks II. Swelling, J. Chem. Phys. 11 (1943) 521–526.

[41] P.J. Flory, J. Rehner Jr., Statistical theory of chain configuration and physical properties of high polymers, Ann. N. Y. Acad. Sci. 44 (1943) 419–429.

[42] L. Leger, C. Creton, Adhesion mechanisms at soft polymer interfaces, Phil Trans R Soc A 366 (2008) 1425–1442.

[43] E. Raphael, P.G. de Gennes, Rubber-rubber adhesion with connector molecules, J. Phys. Chem. 96 (1992) 4002–4007.